Image Clustering Using a Growing Neural Gas with Forbidden Regions

Jesús Benito-Picazo, Esteban J. Palomo, Enrique Domínguez
Department of Computer Languages and Computer Science
University of Málaga
Málaga, Spain
{jpicazo, ejpalomo, enriqued}@lcc.uma.es

Antonio Díaz Ramos
Department of Algebra
University of Málaga
Málaga, Spain
adiazramos@uma.es

***Abstract*—Clustering is one of the most common applications of unsupervised learning, being present in many statistical data analysis processes performed by scientists and engineers. Because of their special features, some categories of Artificial Neural Networks have demonstrated to be specially efficient when it comes to clustering. The Growing Neural Gas (GNG) is a good example of these networks, not only because its capability for revealing the clusters underlying in a certain distribution with an optimized number of neurons, but to faithfully describe the topological relations among the different clusters of a dataset. However, because of their intrinsic nature, there will be some data distributions with regions where no data can be found. Aiming to perform a clustering process on these datasets, this paper presents the design of a Growing Neural Gas-inspired model that keeps its neuron prototypes out of a set of regions previously specified, namely Forbidden Region Growing Neural Gas (FRGNG). Experimental results illustrate how this model can represent an alternative, in terms of accuracy, to one of the most recent region avoiding clustering algorithms such as the Forbidden Region Self-Organizing Map (FRSOFM).**

***Index Terms*—Forbidden regions, Growing Neural Gas (GNG), unsupervised learning, vector quantization**

I. INTRODUCTION

One of the main approaches to represent an input data distribution by describing the relations among the cluster is the Self-Organizing Feature Map (SOFM) proposed originally by Kohonen [1]. Given an input dataset, each neuron of the SOFM learns a representative (centroid) of a subset of the input in order to neurons, which are close in the lattice, adapt to data subsets which are close together.

After the introduction of the SOFM, a myriad of alternatives and derivatives have been proposed in the literature in order to enhance the quality of the mapping or enrich the representation. SOFM-based neural networks that grow during map training have in common that the training starts with a rather small number of units (neurons). New neurons are inserted into the network at certain iterations until a stopping criterion. In some models, links between neurons are being added or removed during training, thus, influencing their neighborhood relations and allowing for a stronger separation of clusters. For instance, the Incremental Grid Growing (IGG) [2] initially consists of four connected neurons in a rectangular grid structure. During the training process, the structure as well as the connectivity of the network is dynamically adapted by adding new neurons at the border of the network adjacent to the neuron having the maximum quantization error, in order to provide more map space for a better representation of the input data. Similarly, during the training of the Growing Cell Structures (GCS) [3], neurons are added and the state of connections changed, but with more freedom regarding the topology of the map space. Growing Neural Gas (GNG) [4] uses a similar algorithm but implements a different learning rule. In the Growing Grid (GG) [5], complete rows and columns of neurons are added to the network maintaining a rectangular grid until the training process is terminated. New neurons are inserted between the neuron with the highest number of hits and its most dissimilar neighbor in terms of weight vector distance, while the connections between the neurons remain untouched. A growing grid variant with an adaptive hyper-cubical output space is presented in [6].

However, in many application or datasets, there are some regions in the input data space where any prototype (centroid) is forbidden. Those forbiden regions, which can represent physical barries, are usually defined by convex polyhedral sets.

Many different algorithms that take into account forbidden regions have been proposed over the years. The problem of locating a new facility in the presence of convex polygonal forbidden regions was addressed in [7], [8]. The same problem with a set of polyhedral barriers that restricts traveling was addressed in [9] and a generalized problem with "congested regions" was treated in [10]. In [11], an algorithm that computes the visibility graph of a set of non-intersecting polygonal obstacles was proposed, and in [12], curved obstacles were considered. Moreover, an integration of a minimal spanning tree (MST) based graph-theoretic technique and expectation maximization (EM) algorithm with rough set initialization was presented for determining non-convex clusters [13]. Recently, a variant of the SOFM, namely the Forbidden Region Self-Organizing Map (FRSOM), whose protoypes avoid those forbidden regions has been proposed [14]. In this paper, a new variant of the GNG, namely the Forbidden Region Growing Neural Gas (FRGNG), whose neuron prototypes avoid the forbidden regions is proposed and compared to the FRSOM.

The rest of paper is organized as follows. Section II presents the mathematical model of our proposal. In Section III, our experimental results are provided. Finally, Section IV concludes

978-1-7281-6926-2/20/$31.00 ©2020 IEEE

this paper.

II. METHODOLOGY

In this work, the matematical base for the new FRGNG algorithm will be constituted by the well known GNG algorithm [4]. In essence, the FRGNG is designed as a GNG algorithm who has the capabilities of avoiding forbidden regions at the moment of a new neuron creation and at the moment the synaptic weights of an existing neuron are modified as a result of the training process. This new feature has been designed based on the the FRSOFM forbidden region avoidance feature explained in [14]. Thus, this section is going to focus in the new region avoidance feature this model incorporates to the original GNG.

So, let $\mathcal{B}$ be a collection of pairwise disjoint convex polyhedral sets $B_1, \ldots, B_N$ located in the space $\mathbb{R}^D$. Each set $B_i \subset \mathbb{R}^D$ is defined as a *barrier*

$$B_i = \text{Conv}(\mathbf{p}_{i,1}, \ldots, \mathbf{p}_{i,n_i}) = \\ = \Big\{ \sum_{j=1}^{n_i} \alpha_j \mathbf{p}_{i,j} | \forall j, \alpha_j \geq 0, \text{ and } \sum_{j=1}^{n_i} \alpha_j = 1 \Big\} \tag{1}$$

where Conv stands for the convex hull of a set of points in $\mathbb{R}^D$.

Given two points spotted outside the set of barriers $\mathcal{B}$, the objective is to compute the shortest path that connects a with b avoiding all barriers. The visibility graph $\mathcal{G}$, is built from all the extreme points of all barriers, $\bigcup_{i=1}^{N} \{\mathbf{p}_{i,1}, \ldots, \mathbf{p}_{i,n_i}\}$, and $\mathcal{G}$ will have an edge between two vertices if they are visible from each other, this is, if the segment between them does not interfere with any of the barriers. In this algorithm, moving along the barriers boundaries is allowed and the weights of the edges are the Euclidean distances between them. Once the graph is constructed, Dijsktra's algorithm will be used to calculate the shortest distance $d_{\mathcal{G}}(\mathbf{p}, \mathbf{q})$ between any pair of vertices, $\mathbf{p}$ and $\mathbf{q}$, of $\mathcal{G}$, just as follows:

(i) First, it will determine the vertices $\{\mathbf{p}_1, \ldots, \mathbf{p}_{n_a}\}$ of $\mathcal{G}$ that are visible from $\mathbf{a}$.
(ii) Second, the algorithm will determine the vertices $\{\mathbf{q}_1, \ldots, \mathbf{q}_{n_b}\}$ of $\mathcal{G}$ that are visible from $\mathbf{b}$.
(iii) Finally, the shortest path and distance $d_{\mathcal{G}}(\mathbf{a}, \mathbf{b})$ are found by optimizing the following expression

$$\min_{i,j}(d(a, \mathbf{p}_i) + d_{\mathcal{G}}(\mathbf{p}_i, \mathbf{q}_j) + d(\mathbf{q}_j, b)), \tag{2}$$

where d is the Euclidean distance in $\mathbb{R}^2$.

In order to properly explain the FRGNG model is very important to define the *Traverse* function. Lets suppose that the shortest path between $\mathbf{a}$ and $\mathbf{b}$ goes through the extreme points of barriers $\mathbf{s}_1, \ldots, \mathbf{s}_n$ and has length d. Then, for $0 \leq c \leq 1$, we define

$$\text{Traverse}(c, \mathbf{a}, \mathbf{b}, \{\mathbf{s}_1, \ldots, \mathbf{s}_n\}) \tag{3}$$

as the point located along this shortest path at a distance from $\mathbf{a}$ which is a fraction c of the total distance d.

So, the Forbidden Region GNG that will be referred as FRGNG through all this document will update q and all its direct topological neighbors with step size ϵ_b for unit r and ϵ_n for the neighbors, where $\epsilon_b > \epsilon_n$:

$$\epsilon(n, i) = \begin{cases} \epsilon_b & \text{iff } i == r \\ \epsilon_n & \text{iff } (i \neq r) \wedge (i, r) \in A \\ 0 & \text{iff } (i \neq r) \wedge (i, r) \notin A \end{cases} \tag{4}$$

$$\mathbf{w}_i(n+1) = (1 - \epsilon(n, i))\, \mathbf{w}_i(n) + \epsilon(n, i)\, \mathbf{x}_t \tag{5}$$

This equation will be equivalent to

$$w_i(n+1) = Traverse(\epsilon(n, i), w_i(n), x(n),) \tag{6}$$

So, assuming that $D = 2$ and being $\mathbf{s}_1, \ldots, \mathbf{s}_n$ the breaking points of the the shortest path from $\mathbf{w}_i(n)$ to $\mathbf{x}(n)$ that avoids the barriers, $\mathcal{B}$, the new update function for the neuron prototypes will be:

$$\mathbf{w}_i(n+1) = Traverse(\epsilon(n, i), w_i(n), x(n), s_1, s_2, \cdots, s_n) \tag{7}$$

This operating mode will avoid the movement of neurons across the forbidden regions of the feature vector scape. However, since we are using the GNG model as the base for the FRGNG, once the neuron prototypes have been updated it may be necessary to add a new neuron if the current time step is a multiple of the λ parameter. Nevertheless, as no rule in the mathematical mode is preventing this to happen there is a real chance that the new neuron "spawns" inside one of the barriers of $\mathcal{B}$. Hence, the new neuron will be generated as follows:

- First, determine the unit r with the maximum error and the unit z with the largest error among all direct neighbors of r.
- Then create a new unit k, insert edges connecting k with r and z, and remove the original edge between r and z.
- After that, decrease the error variables e_r and e_z by multiplying them with a constant α, and initialize the error variable e_k to the new value of e_r.
- Next, setup the prototype of k to be halfway between those of r and z, as follows:

$$\mathbf{w}_k(n) = \frac{1}{2}(\mathbf{w}_r(n) + \mathbf{w}_z(n)) \tag{8}$$

- Finally, if the new neuron k is generated inside a barrier, the new prototype vector of this neuron will be:

$$\mathbf{w}_k(n) = (x_s, y_s) \tag{9}$$

where (x_s, y_s) will be the prototype vector of the sample whose euclidean distance to the k neuron is the shortest.

TABLE I
NUMBER OF SAMPLES FOR EACH BIOGEOGRAPHIC DATASET.

Species	Region of interest	Number of samples
Tiger shark	Australia	481
Dolphinfish	Australia	1405
Blue Shark	Australia	1541
Common dolphin	Celtic and North Seas	2813
Fin whale	Greenland and Iceland	734

III. EXPERIMENTAL RESULTS

In order to test the new Forbidden Region Growing Neural Gas performance applied to data distribution clustering tasks and its capability for representing the topological relations between the different clusters, a complete set of tests has been designed. These tests involved data distributions corresponding to real events happened in different geographical locations on the surface of the earth. As it has been explained before, because of their intrinsic nature, these events present circumstances that made them impossible to happen in determined geographical locations.

Thus, five datasets have been used through all the experimental process. These datasets are composed by biogeographical data consisting of bi-dimensional number vectors representing the latitude and longitude coordinates of real sightings of marine animals. Three of them in the surroundings of the Australian mainland: Blue shark, tiger shark and common dolphinfish. One around the Celtic and North Seas: the common dolphin. The last dataset corresponds to the sightings of the fin whale around Greenland and Iceland. Because of obvious reasons, no marine species can be seen in mainland, so the mainland areas of the different geographical zones will constitute the forbidden regions for our experiments. Every dataset has been obtained from the free and open access OBIS (Ocean Biogeographic Information System, www.iobis.org) database and their characteristics can be consulted in Table I and Figure 1:

A. Experiments design

The experimental process consisted of training a FRGNG model instance for a final number of 4, 16, 36 and 64 neurons. Note that we use the word "final" for the number of neurons of the FRGNG because this model is a network that grows along the training process. As a competitor for the FRGNG model presented in this work, it has been considered the FRSOFM model from [14]. Thus, The experiments also included the training of a FRSOFM network for 4, 16, 36, and 64 neurons with square topology so both models can be compared. The results of this training process can be seen in Figure 2 where the final distributions of neurons for each model, dataset and number of neurons are illustrated.

In order to design an experiment as reproducible as possible, and with the objective of reducing the number of possible configurations of the system that in other way would grow to be unmanageable, both models have been trained using the same values through all the experimentation process. For both the FRGNG and the FRSOFM models, the values for the parameters can be consulted in tables II and III.

TABLE II
SELECTED PARAMETER VALUES FOR THE FRGNG MODEL.

Parameter	Value
ϵ_b	0.2
ϵ_n	0.000001
a_{max}	50
λ	variable
H_{max}	4-64
α	0.5
d	0.995

TABLE III
SELECTED PARAMETER VALUES FOR THE FRSOFM MODEL.

Parameter	Value
η_0	0.441
Δ_0	0.5597
η_c	0.1669
Δ_c	0.3077

It is very important to remark that the training parameter values for the FRSOM model are the same as the ones mentioned in [14]. Those parameter values were specifically optimized by the authors for the datasets used. In contrast to this, training parameters for the FRGNG were not specifically optimized for the datasets. For this new model, a generic parameter selection, derived from the parameters used in [4], has been done whithout any kind of optimization process.

As it is usual in this kind of experiments, in order to obtain significant results, and aiming to carry out a rigorous experimentation process, each algorithm has been tested by performing a 10-fold cross-validation process for every model, dataset and number of neurons. By means of this process, the mean values of three commonly used clustering quality performance measures have been obtained: The Davies-Bouldin Index (DBI), the Mean Squared Error (MSE) and the Dunn Index.

Davies Bouldin Index has been calculated following the following expression:

$$DB = \frac{1}{n_c}\sum_{i=1}^{n_c} R_i$$

Where

$$R_i = \max_{j=1\cdots n_c, i\neq j}(R_{ij}), i = 1\cdots n_c$$

$$R_{ij} = \frac{s_i + s_j}{d_{ij}}$$

$$d_{ij} = d(v_i, v_j), s_i = \frac{1}{\|c_i\|}\sum_{x\epsilon c_i} d(x, v_i)$$

Being $d(x, y)$ the Euclidean distance between x and y. c_i will be the $i-th$ cluster. v_i is the centroid of cluster c_i and $\|c_i\|$ refers to the norm of c_i.

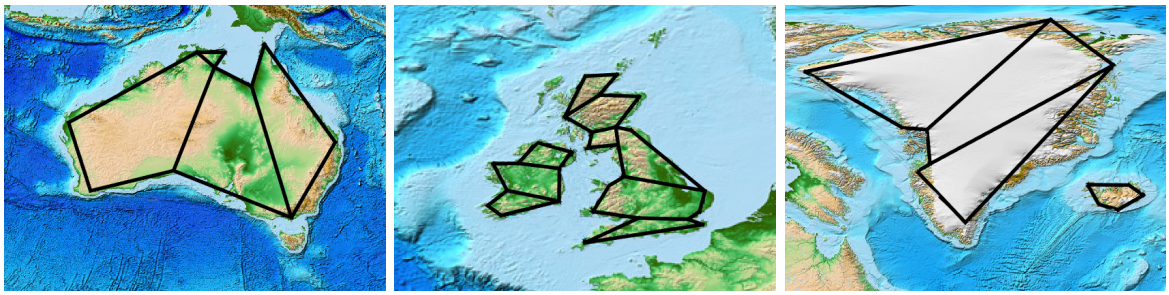

(a) (b) (c)

Fig. 1. Geographical locations for the datasets and their equivalents in polygonal barriers : (a) Australia, (b) Celtic and North Seas, (c) Greenland and Iceland.

TABLE IV
RESULTS YIELDED BY THE EXPERIMENTS FOR THE FIVE DATASETS SHOWING THE MEAN VALUES OF THE DBI (LOWER IS BETTER), THE MSE (LOWER IS BETTER) AND DUNN INDEX (HIGHER IS BETTER) FOR 4 NEURONS.

Dataset	Model	DBI	MSE	Dunn
Blue Shark	**FRGNG**	0.4647	8.5148	1.4011
	FRSOFM	0.3995	23.1381	1.8237
Dolphinfish	**FRGNG**	0.5472	7.8524	0.9965
	FRSOFM	0.4361	18.1298	1.6034
Tiger Shark	**FRGNG**	0.5744	2.7439	0.3324
	FRSOFM	0.4171	30.4653	1.6208
Dolphin	**FRGNG**	0.8934	3.5314	0.7040
	FRSOFM	0.7178	4.0852	1.2945
Whale	**FRGNG**	0.7281	1.2490	0.4292
	FRSOFM	0.4212	6.4255	1.4772

TABLE V
RESULTS YIELDED BY THE EXPERIMENTS FOR THE FIVE DATASETS SHOWING THE MEAN VALUES OF THE DBI (LOWER IS BETTER), THE MSE (LOWER IS BETTER) AND DUNN INDEX (HIGHER IS BETTER) FOR 16 NEURONS.

Dataset	Model	DBI	MSE	Dunn
Blue Shark	**FRGNG**	0.7069	0.9662	0.5105
	FRSOFM	0.6033	3.1732	0.9485
Dolphinfish	**FRGNG**	0.7245	0.9336	0.2545
	FRSOFM	0.6471	3.6058	0.4095
Tiger Shark	**FRGNG**	0.5967	0.1819	0.3128
	FRSOFM	0.5367	5.4706	0.6776
Dolphin	**FRGNG**	0.7046	0.4469	0.4349
	FRSOFM	0.5928	0.7620	0.5967
Whale	**FRGNG**	0.6955	0.1205	0.0777
	FRSOFM	0.5678	1.0366	0.4128

The Mean Squared Error is another classic performance measure in machine learning which is defined as follows:

$$MSE = \frac{1}{M}\sum_{i=1}^{M}\|\mathbf{w}_i - \mathbf{x}_i\|^2 \tag{10}$$

where M is the number of samples in the dataset, $\mathbf{x}_i$ is the i-th input sample and $\mathbf{w}_i$ is the prototype of the winning neuron corresponding to x_i.

Introduced by J. C. Dunn in 1974, the Dunn index is a commonly used measure for evaluating clustering quality that is calculated by applying the following expression for a number c of clusters:

$$Dunn = \min_{1\leq i\leq c}\left(\min_{1\leq j\leq c, j\neq i}\left(\frac{\delta(X_i, X_j)}{\max_{1\leq k\leq c}(\Delta(X_k))}\right)\right)$$

Where $\delta(X_i, X_j)$ is the intercluster distance. This is, the distance between the cluster i and the cluster j, and $\Delta(X_k)$ is the intracluster distance, this is, the distance within the cluster X_k.

Once the experiments were performed, the results obtained for each dataset, number of neurons and model for every of the above explained indexes, can be checked in tables IV, V, VI and VII.

At the same time, the evolution of the results obtained for the DBI, MSE and Dunn index for each dataset as the final number of neurons grows is illustrated in Figure 3.

TABLE VI
RESULTS YIELDED BY THE EXPERIMENTS FOR THE FIVE DATASETS SHOWING THE MEAN VALUES OF THE DBI (LOWER IS BETTER), THE MSE (LOWER IS BETTER) AND DUNN INDEX (HIGHER IS BETTER) FOR 36 NEURONS.

Dataset	Model	DBI	MSE	Dunn
Blue Shark	**FRGNG**	0.7525	0.3443	0.3461
	FRSOFM	0.6115	1.5457	0.5976
Dolphinfish	**FRGNG**	0.7094	0.3028	0.3641
	FRSOFM	0.6061	1.4917	0.2657
Tiger Shark	**FRGNG**	0.5206	0.0371	0.3671
	FRSOFM	0.5442	1.8987	0.3975
Dolphin	**FRGNG**	0.6877	0.1568	0.1215
	FRSOFM	0.6222	0.3550	0.2436
Whale	**FRGNG**	0.6802	0.0369	0.1106
	FRSOFM	0.6608	0.5122	0.2437

B. Discussion

Values yielded by the experimental process can be checked in both Figure 3 and tables from 1 to 4. On them, it can be observed the behaviour of the FRGNG when trained and tested with the five different bi-dimensional data distributions that have been used as datasets. It also can be observed the behaviour of the model it has been used as a competitor, the FRSOFM, when trained with the same datasets.

Charts of the first column of Figure 3 represent the DBI, MSE and Dunn index values for the two models and the dataset corresponding to the blue whaler shark. These charts reveal how the FRGNG values for the MSE performance measure are

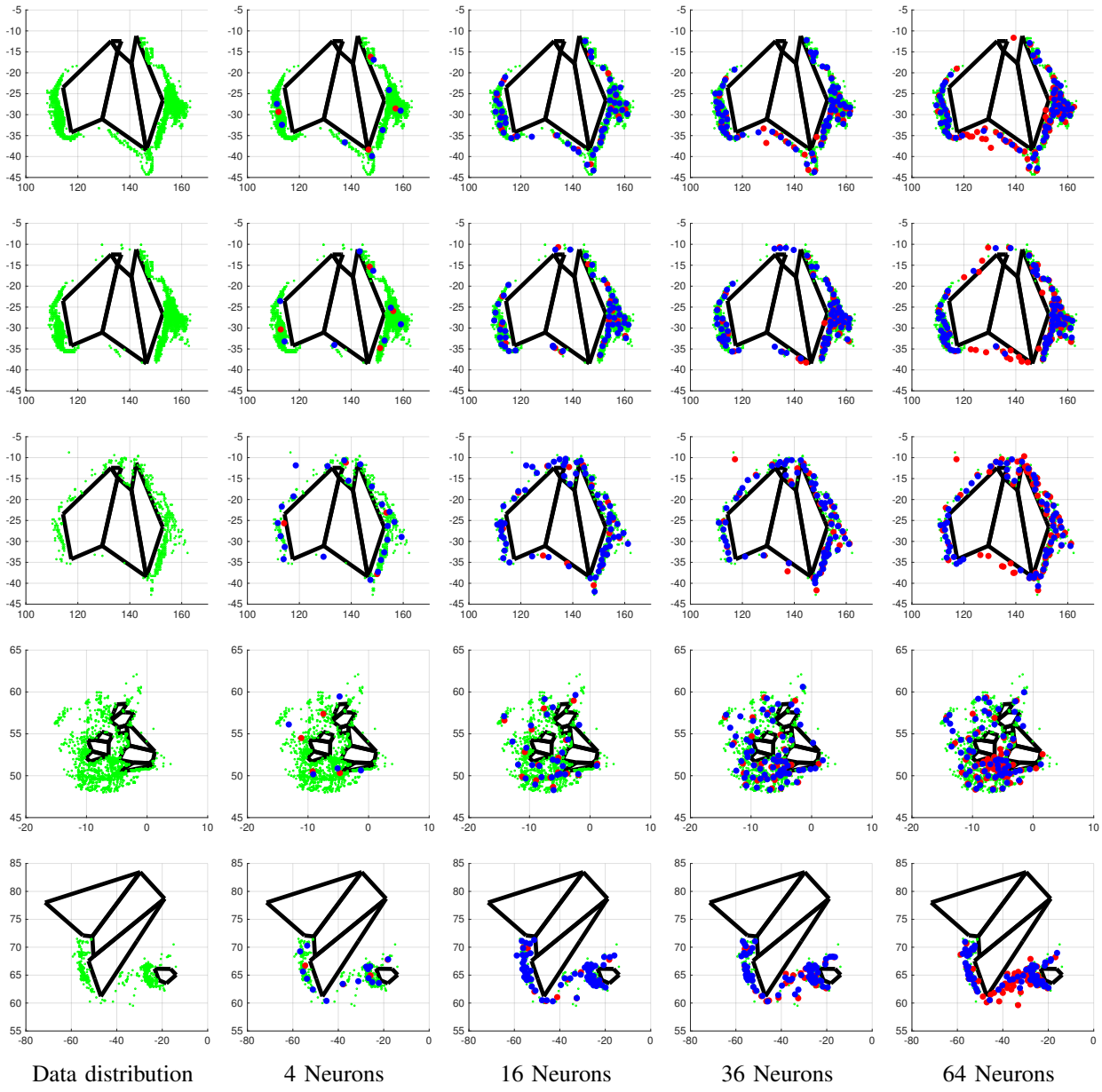

Fig. 2. Final locations for FRSOFM and FRGNG neurons on the different datasets. Respectively, in rows from 1 to 5: blue shark, dolphinfish, tiger shark, common dolphin and fin whale. Green spots correspond to samples in the data distribution. Blue circles correspond to FRGNG neurons. Red circles correspond to FRSOFM neurons.

significantly below the FRSOFM values. However, its Dunn index values are also below the FRSOFM values for every number of neurons and the DBI value for this dataset is higher than the DBI value for the FRSOM. Nevertheless, as all the measures are in the same magnitude order, we can conclude that for the blue whaler shark dataset, both methods perform very similarly.

When it comes to the dolphinfish sightings around the australian coast dataset, the scores reached by the experiments are as significant as in the dataset above insofar as the MSE index for the FRGNG value is better than the value for the same measure reached by the FRSOM. However, the DBI value obtained by the FRSOM is better in this case than the DBI value presented by the FRGNG for all neuron numbers. In the case of the Dunn index we can observe that it is better for the FRSOFM except for the value associated to the 36 neurons map, where the FRGNG gets the best value.

Results are even more balanced for the Tiger shark sightings on the surroundings of the coast of Australia. In the case of this dataset, the DBI value is better for the FRSOM for 4 and 16 neurons maps. However, this circumstance changes for 36 and 64 neurons where the values reached by the FRGNG are better. In the case of the MSE index, FRGNG values are better with no exception. When it comes to the Dunn Index, results illustrate that the FRSOM has a better performance for this dataset.

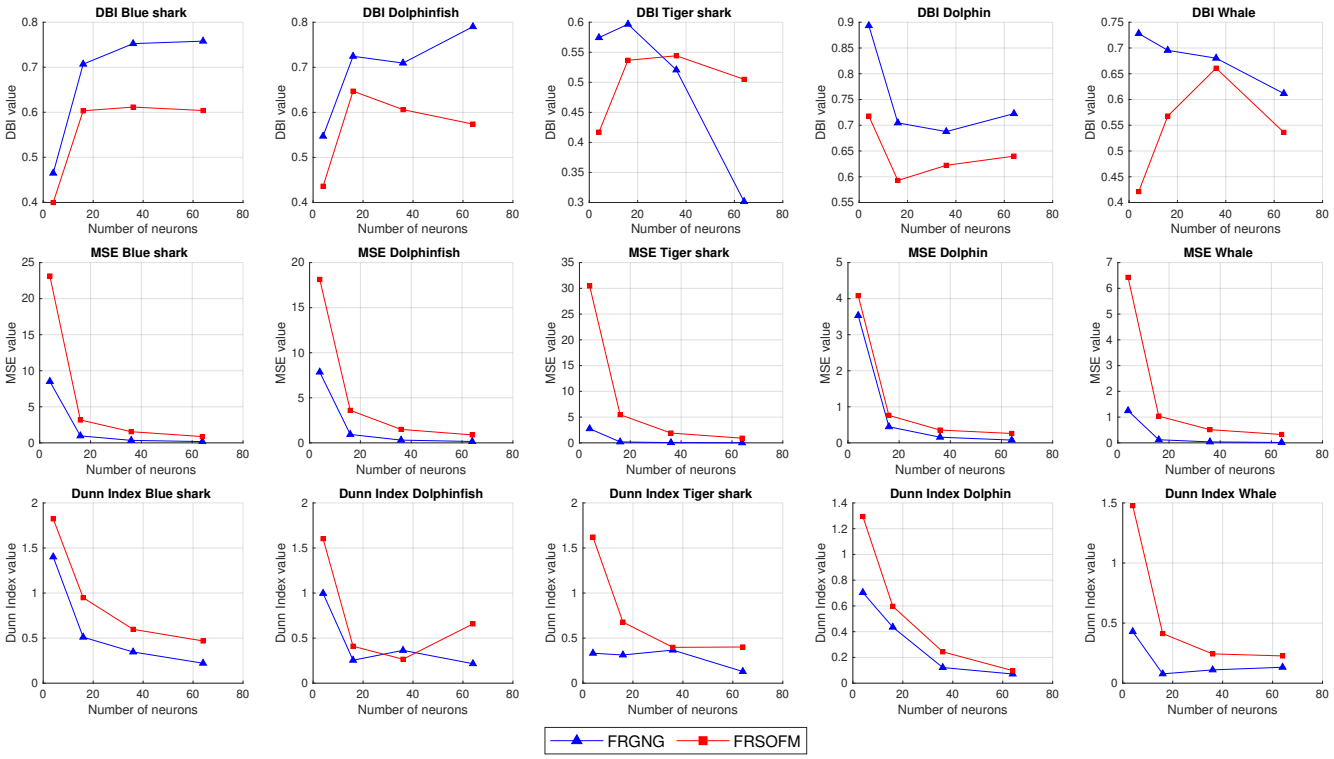

Fig. 3. Comparative results for DBI, MSE and Dunn Index obtained after the experimentation process by FRSOFM and FRGNG on the different datasets.

TABLE VII
RESULTS YIELDED BY THE EXPERIMENTS FOR THE FIVE DATASETS SHOWING THE MEAN VALUES OF THE DBI (LOWER IS BETTER), THE MSE (LOWER IS BETTER) AND DUNN INDEX (HIGHER IS BETTER) FOR 64 NEURONS.

Dataset	Model	DBI	MSE	Dunn
Blue Shark	**FRGNG**	0.7580	0.1738	0.2215
	FRSOFM	0.6039	0.8698	0.4684
Dolphinfish	**FRGNG**	0.7902	0.1503	0.2163
	FRSOFM	0.5740	0.8823	0.6577
Tiger Shark	**FRGNG**	0.3016	0.0073	0.1294
	FRSOFM	0.5050	0.9054	0.4014
Dolphin	**FRGNG**	0.7226	0.0764	0.0713
	FRSOFM	0.6400	0.2597	0.0975
Whale	**FRGNG**	0.6116	0.0145	0.1325
	FRSOFM	0.5362	0.3245	0.2269

Experimental results obtained by the FRGNG in the case of the common dolphin over the Celtic and North seas dataset are in the same spirit as the results obtained for the blue whaler shark dataset. This is, FRGNG performance is better than the FRSOFM when considering the MSE measure, whilst FRSOM DBI and Dunn index are better than the DBI and Dunn index reached by the FRGNG for every neurons number map.

Finally, scores reached by the FRGNG when tested against the FRSOFM with the fin whale over the surroundings of the coast of Greenland and Iceland dataset illustrate, once again, how the FRGNG clustering quality is very similar to the clustering quality obtained by the FRSOFM. However, in this case, looking at the chart represented on the 1st row and 5th column of the Figure 3, it can be observed that the DBI values for both models present different trends for 4 to 36 neurons maps: The FRGNG DBI value presents a descending curve whilst the FRSOM presents an ascending curve. Both curves turn descending from 36 to 64 neurons maps. Once more, the MSE value for the FRGNG remains lower than the MSE value reached by the FRSOM and the Dunn index is slightly better for the FRSOM map.

Overall, data represented in tables 4 to 7 and the representations in Figures 2 and 3 illustrate how the clustering quality and topology representation faithfulness achieved by the two models are similar. However, FRSOM model often seems to win when it comes to the DBI and Dunn index measures, while the FRGNG model presents better MSE values. This is a very interesting behaviour given the fact that the parameters of the FRGNG model have not been optimized for the datasets while the parameters for the training of the FRSOM have indeed been optimized for the datasets.

IV. CONCLUSION

In this work, a new artificial neural network-based model has been presented for unsupervised data clustering. This model is designed for data clustering processes with data distributions where there are some regions of the feature vector space where no data can be found. Combining the plasticity of the Growing Neural Gas model and the ability of the FRSOFM model for avoiding the forbidden regions, this model is capable of achieving a similar performance as its best competitor, the Forbidden Region Self-Organized Map (FRSOFM), despite the

fact that, unlike the FRSOM, its training parameters have not been specifically optimized for the datasets.

Experimental results illustrate the FRGNG performance against the FRSOFM model, remarking their similar behaviour for almost every considered size in every considered dataset, postulating the FRGNG as a very powerful mathematical model for data clustering and cluster topology representation.

ACKNOWLEDGMENT

This work is partially supported by the Ministry of Economy and Competitiveness of Spain under grants TIN2016-75097-P and PPIT.UMA.B1.2017. It is also partially supported by the Ministry of Science, Innovation and Universities of Spain under grant RTI2018-094645-B-I00, project name Automated detection with low-cost hardware of unusual activities in video sequences. It is also partially supported by the Autonomous Government of Andalusia (Spain) under project UMA18-FEDERJA-084, project name Detection of anomalous behavior agents by deep learning in low-cost video surveillance intelligent systems. All of them include funds from the European Regional Development Fund (ERDF). The authors thankfully acknowledge the computer resources, technical expertise and assistance provided by the SCBI (Supercomputing and Bioinformatics) center of the University of Málaga. They also gratefully acknowledge the support of NVIDIA Corporation with the donation of two Titan X GPUs used for this research. The authors acknowledge the funding from the Universidad de Málaga.

REFERENCES

[1] T. Kohonen, "The self-organizing map," *Proceedings of the IEEE*, vol. 78, no. 9, pp. 1464–1480, 1990.

[2] J. Blackmore and R. Miikkulainen, "Incremental grid growing: encoding high-dimensional structure into a two-dimensional feature map," in *IEEE International Conference on Neural Networks*. IEEE, 1993, pp. 450–455.

[3] B. Fritzke, "Growing cell structures - A self-organizing network for unsupervised and supervised learning," *Neural Networks*, vol. 7, no. 9, pp. 1441–1460, 1994.

[4] ——, "A Growing Neural Gas Network Learns Topologies," *Advances in Neural Information Processing Systems 7*, vol. 7, no. 1, pp. 625–632, 1995.

[5] ——, "Growing Grid - a self-organizing network with constant neighborhood range and adaptation strength," *Neural Processing Letters*, vol. 2, no. 5, pp. 9–13, 1995.

[6] H. U. Bauer and T. Villmann, "Growing a hypercubical output space in a self-organizing feature map." *IEEE transactions on neural networks*, vol. 8, no. 2, pp. 218–26, 1997.

[7] S. E. Butt and T. M. Cavalier, "An efficient algorithm for facility location in the presence of forbidden regions," *European Journal of Operational Research*, vol. 90, no. 1, pp. 56 – 70, 1996.

[8] R. G. McGarvey and T. M. Cavalier, "A global optimal approach to facility location in the presence of forbidden regions," *Computers & Industrial Engineering*, vol. 45, no. 1, pp. 1 – 15, 2003.

[9] K. Klamroth, "A reduction result for location problems with polyhedral barriers," *European Journal of Operational Research*, vol. 130, no. 3, pp. 486 – 497, 2001.

[10] M. S. Farham, H. Süral, and C. Iyigun, "Generalization of the restricted planar location problems: Unified metaheuristic algorithms," *Computers & Operations Research*, vol. 99, pp. 48 – 66, 2018. [Online]. Available: http://www.sciencedirect.com/science/article/pii/S0305054818301138

[11] S. K. Ghosh and D. M. Mount, "An output-sensitive algorithm for computing visibility graphs," *SIAM Journal on Computing*, vol. 20, no. 5, pp. 888–910, 1991.

[12] D. Z. Chen and H. Wang, "Computing shortest paths among curved obstacles in the plane," in *Symposium on Computational Geometry*, 2013.

[13] P. Mitra, S. K. Pal, and M. A. Siddiqi, "Non-convex clustering using expectation maximization algorithm with rough set initialization," *Pattern Recognition Letters*, vol. 24, no. 6, pp. 863 – 873, 2003.

[14] A. Díaz Ramos, E. López-Rubio, and E. J. Palomo, "The forbidden region self-organizing map neural network," *IEEE Transactions on Neural Networks and Learning Systems*, pp. 1–11, 2019.